ROOM
-VENT
'90

Similitude modeling of nonisothermal air flow in rooms with internal obstructions

B1

L. Christianson
J. Zhang
G. Wu
G. Riskowski
University of Illinois, Urbana, Illinois , USA

SIMILITUDE MODELING OF NONISOTHERMAL AIR FLOW IN ROOMS WITH INTERNAL OBSTRUCTIONS

L. Christianson, J. Zhang, G. Wu, G. Riskowski[1]
University of Illinois
Urbana, Illinois USA

Understanding room air and air contaminant distribution is essential to the design of a ventilation system and the control of room thermal and air quality conditions. The importance of this is summarized in the findings of the recent symposium Building Systems: Room Air and Air Contaminant Distribution (Christianson, 1989), "The movement of air within a room directly affects the air quality ... and determines how these pollutants affect people. Several industries and emerging technologies depend in part on room air and air contaminant distribution expertise. Major industries including clean room manufacturing, electronic and computer rooms, biomedical research, hospital disease control, and greenhouse and animal agriculture, rely on advances in contaminant control to remain competitive".

Room air and air contaminant distribution is a complicated process. Researchers have developed a limited understanding through experimental measurements and numerical modeling. Research efforts have concentrated on high ventilation conditions (fully turbulent flow), isothermal conditions (no internal heat loads), limited if any internal obstructions (no furniture and equipment), and simple room geometries because of the complexity of the problems.

Advances in numerical modeling techniques coupled with the importance of addressing realistic room conditions have encouraged researchers to begin developing low turbulent, non-isothermal models which can handle more realistic room conditions such as low turbulent, non-isothermal airflow (Baker and Kelso, 1989; Murakami, 1989; Nielsen, 1989; Ferziger, 1989). However, these researchers are limited by the availability of detailed room air movement data, particularly for full-scale rooms. They are also limited by our inability to scale data to compare reduced and full-scale rooms and different sized rooms.

Our objectives are to:

(1) Investigate the regional airflow characteristic of a realistic ventilated room, especially with obstructions, with heat sources, with both obstructions and heat sources, and under low turbulence airflow conditions.
(2) Develop a method for scaling among different sized rooms.
(3) Provide experimental data for the analysis and evaluation of theoretically-based models of room air and air contaminant distribution in ventilated rooms.

---

[1]The authors are Associate Professor, Research Assistant, Research Associate and Assistant Professor in Agricultural Engineering at the University of Illinois, Urbana-Champaign, U.S.A.

Literature Review

Problem Significance

Methods commonly used for studying room air and air contaminant movement are prototype measurements, scale model measurements coupled with similitude analysis, and numerical simulation. Prototype study is limited because results are only directly applicable to rooms and environmental conditions identical (or at least very similar) to that originally studied.

Similitude study is limited because distortion is necessary for the most realistic situations (i.e., low turbulent flow where thermal buoyancy and internal obstructions are important). Researchers have documented that undistorted similitude models can be developed for certain classes of conditions (e.g., plug flow and laminar, isothermal flow). Similitude models are useful for scaling ventilation system designs, based on data from one sized room, to different sized but similar rooms. However, a generalized scaling method is not available at present.

Recently, researchers have tried the numerical simulation methods to predict room airflow and air contaminant distribution for more realistic situations, however, their efforts to develop and evaluate the numerical models are limited by the availability of detailed data, which describe three-component air velocities, temperature, pressure, and turbulent structure throughout the room. Such data for realistic room conditions, either for reduced-scale or full-scale, are especially limited. Therefore, there is little confidence that any of these models can be applied to the practical design of ventilation systems and control of room environments.

Similitude Model Studies

Similitude studies are conducted by measuring environmental parameters in reduced-scale model rooms and extrapolating the experimental results to full-scale prototypes based on the similitude theory.

Few similitude studies of air distribution for the residential and commercial rooms have been done. Baturin (1972) describes similitude modeling for room air, using air as the modeling fluid, and cites examples from several Russian engineers.

Moog (1981) provided a phenomenological description and physical analysis of a room flow. It was pointed out that complete similarity was impossible in conducting reduced scale model tests due to the complexity of the room flow. Partial similarity was usually used in which only the relatively important dimensionless parameters were maintained undistorted while the others were distorted. For example, the Archimedes number could be used as the single critical dimensionless parameter for scaling experiments of laminar flow which is mainly affected by thermal buoyancy and inertial force (a simplification allowed for vertical displacement room flows).

More similitude work has been done using water (rather than air) as the working fluid in the model to simplify scaling in experiments. Anderson and Mehos (1988) used water as the working fluid in a 1/4th scale test cell to evaluate indoor air pollutant control techniques by measuring the distribution of flow velocities and pollutants. The tests were designed based on Reynolds number criterion and are limited to isothermal flows. Velocity measurements of a wall jet in the test cell were compared with previous full scale measurements of a wall jet to confirm the accuracy of their scaling approach based on Reynolds number. However, there was no comparison between the velocities throughout the test cell with corresponding full scale measurements. Thus, it was not properly justified that using Reynolds number as a single scaling parameter was appropriate for studying the entire room flow field.

Agricultural engineers have used similitude methods extensively to study ventilation of animal rooms. Pattie and Milne (1966) used an 1/10th scale model to study the airflow pattern and air velocity distribution in a broiler house with tube diffusers on one sidewall and an exhaust fan centered on the other. All the tests were done in an empty room (i.e., no internal obstructions) and the inside temperature was approximately equal to the outside air temperature (i.e., isothermal conditions). They defined a theoretical air velocity as the ratio of ventilation rate to the area of the cross-section, which is parallel to the sidewalls. A non-dimensional air velocity was obtained by dividing the air velocity by the theoretical velocity. They concluded that the airflow was practically 2-dimensional, and the airflow pattern and the non-dimensional air velocity distribution were independent of Reynolds number for a certain range (0.2-0.91 based on the diffuser hole diameter in their study) of Reynolds number values.

Furry and Hazen (1967) investigated the applicability of the similitude principles to the prediction of the concentration of gas constituents in a confined, ventilated space with no internal heat loads and obstructions. Their experimental results indicated that neither the Froude number (ratio of inertial force to gravity) nor the Reynolds number (ratio of inertial force to viscous force) appeared to impose contradictory requirements for modeling the gas-dilution phenomenon, though it is apparent that they were contradictory in predicting the air velocity.

Timmons (1984a) used a reduced-scale model to evaluate the effect of diffuser slot width and diffuser location (having a diffuser on only one sidewall versus on each sidewall) on the internal air velocities in an empty room under isothermal conditions. He defined a non-dimensional air velocity to be the ratio of air velocity to the average diffuser velocity (ventilation rate divided by total diffuser area), which was assumed to be identical for any scale models or prototypes in fully developed turbulent flow cases. He concluded that the non-dimensional velocity was negatively related to the ratio of (room cross sectional area)$^{1/2}$ to slot width and that there were no significant differences in overall mean velocity between using two continuous slot diffusers (each of width D/2 employed on opposite walls) and a single continuous slot diffuser of width D.

Timmons (1984b) also compared the results from the similitude model to that measured in a prototype, indicating excellent agreement in predicting airflow patterns and velocity profiles for the case of fully developed turbulent flow.

He also showed that the threshold Reynolds number, above which the dimensionless velocity and flow pattern were independent of Reynolds number, increases with the size of a model or prototype. However, the relation between the threshold Reynolds number and room scales was not developed due to the lack of detailed experimental data.

Preliminary studies at the University of Illinois (Yao et.al. 1986) started with a 1/12th scale swine growing barn with a realistic ventilation rate (which results in low turbulent flow). The similitude analysis also considered the effects of internal heat load (by simulated pigs) and obstructions (pens and simulated pigs). Experimental results indicated that more closely spaced room diffusers (3m air throw versus 6m) provided lower air velocities at the pig level for the same winter ventilation rate. This result is different from Timmons' (1984a), indicating that the effects of internal heat loads and obstructions, and the low turbulence effect are significant. It was also noted that the location of the air exhaust from the room had no noticeable effect on pig-level air velocities. Continuing this work, Christianson et.al. (1988) measured pig-level air velocities in a swine barn which has a similar pen arrangement as that in the model. Comparisons between the field data and that predicted by the similitude model indicated that the Archimedes number appeared to be the more critical independent dimensionless variable compared to the Reynolds number, for predicting room air distribution in swine buildings which use mechanical ventilation systems. However, the unavoidable distortion of the similitude model has to be corrected before it can provide accurate predictions for designers.

The above agricultural engineering work is very useful to the study of room air and air contaminant distribution problems in residential and commercial rooms due to the enough similarities between them (Table 1).

Table 1. Comparison Between Typical Agricultural and Residential/Commercial Room Air Diffusers.

	Agricultural	Residential/commercial
Total vent rate[2] (ach)	5 to 60	1 to 15
Internal heat load (W/m^2)	30 to 300	30 to 250
Diffuser velocity (m/s)	2.5 to 50	2.5
Temperature difference (°C)	-60 to +3	+12 to -12
Fresh air supply (ach)	5 to 60	0.5 to 2
Diffuser location	ceiling	ceiling or floor
Heat location	usually floor	mixed

Experiments in reduced scale rooms are generally more convenient and less expensive to conduct, and experimental conditions can be well controlled. However, a proper scaling method is needed to account for the unavoidable distortion in the experiments in order to make the data useful to different sized rooms quantitatively as well as qualitatively. Developing a scaling method for tests of realistic room conditions has been identified as one of research needs

[2] Total ventilation rate refers to fresh plus recirculated airflow rate.

in the current study of room air and air contaminant distribution (Int-Hout, 1989).

Procedures

Field Measurements and Observation

All measurements were made in production swine rooms with approximate dimensions of 11.6 x 9.1 x 2.1 m. The ventilation rate was approximately 5 to 10 air changes per hour. Air velocities were measured at 17 points in the center section of one room without pigs inside using an omni directional, temperature compensated hot wire anemometer; then mean and standard deviation were calculated for each point. Smoke generated by heating mineral oil with a pesticide fogger was used to visualize the flow pattern in the building. In addition, flow patterns were visualized with the smoke method in another swine nursery room and two swine finishing rooms with pigs inside (Pigs are the primary internal heat source in swine rooms). All smoke patterns were recorded with a video camera. These field measurements revealed a general airflow pattern typical of mechanically ventilated swine rooms in cold and mild weather.

Reduced-Scale Physical Model Study

The 1/12th scale-model building (1092 × 914 × 203 mm) used by Yao et al. (1986) and Christianson et al. (1988) was modified for detailed study of regional flow characteristics (Figure 1). The model building (chamber) had a continuous slot air diffuser and a continuous slot exhaust, both as long as the side walls,[3] so that the flow inside was essentially two-dimensional. Water from the adjustable setting, constant-temperature water bath was pumped through the uniformly distributed plastic pipes on the floor to simulate an internal heat load. Both the ventilation rate and the diffuser air velocity were controlled by adjusting a valve on the air supply duct. The diffuser air velocity was also adjusted by changing the diffuser opening width[4] while keeping the ventilation rate unchanged.

Mean air velocity and temperature were measured at 60 points (a 5 × 12 grid) in the center section of the model room for seven different testing conditions, using an omni directional, temperature-compensated hot wire anemometer and a copper-constantan thermocouple, respectively. The flow was maintained at steady state during the measurements.

Smoke generated by electrically heating a mineral oil coated on a thin wire was used to visualize the airflow pattern in the model building. A video camera was used to record all the flow patterns for comparisons.

---

[3] Both slots have two supports which blocks only 6% of the opening area.

[4] Some authors call it opening height, since the diffuser is on a side wall and the width of opening is the vertical size of the slot.

Based on the measurements and flow pattern visualization in the reduced-scale model building, the effects of thermal buoyancy, diffuser opening width, and ventilation rate on the room air distribution were analyzed. The relationships between the decay rate of maximum jet velocity, the velocity in the occupied zone, and the Archimedes number were established.

Results of Field Measurements and Observation

Figure 2 shows the observed airflow pattern with the measured means and standard deviations of the velocities on the center section of a 11.6 x 9.1 x 2.1 m unoccupied room. Three distinct flow regions were shown: (1) near the diffuser, (2) in the middle, and (3) near the room exhaust on the opposite wall.[5] Air velocities were relatively higher in region 1, which was characterized by a ceiling jet and a large recirculating eddy. In region 2, air traveled with relatively low airspeed. In region 3, air was accelerated due to the contraction of the exhaust. The higher standard deviations in region 1 might indicate that flow in this region was more turbulent compared to regions 2 and 3 where flow acted more like potential flows. The pen partitions had a significant effect on the airflow distribution and resulted in very low air velocities at points 7, 10, 12, and 14 in regions 2 and 3.

Similar airflow patterns were observed in three other rooms, similar in design, with pigs inside. During the observations, the air was introduced into the building from a continuous slot diffuser on one side wall and exhausted by fan(s) on the other side. It was noted that the thermal buoyancy due to the heat generated by pigs appeared to increase the velocities right above the pigs in the low air velocity region (region 2 in Figure 2). The movement of pigs increased the fluctuation of the air velocities in their immediate vicinity but apparently did not affect the overall airflow pattern within the buildings.

Timmons (1984b) reported a secondary recirculating eddy rotating in the opposite direction of the main eddy in measurements of a similar room, but this secondary eddy was not observed in the present study. Perhaps this is because of a much lower diffuser Reynolds number (Re=4,500 to 9,000, corresponding to U_i=2.8 m/s to 3.6 m/s and w_i=2.54 cm to 3.8 cm) in the rooms we studied, compared to Re=54,000 (corresponding to U_i=5.7 m/s and w_i=15.2 cm) in Timmons' (1984b) work.

The present study, combined with findings reported by previous researchers, suggests that flow in slot ventilated buildings generally has the following five types of subfields (Figure 3)

[1] Turbulent jet;
[2] Recirculation flow;
[3] Potential flow;
[4] Exhaust (region in immediate vicinity of exhaust); and
[5] Boundary layers on solid surfaces of the walls and obstructions.

---

[5] These were not intended to be subfields as discussed elsewhere in this paper.

where, subfields [1] and [2] correspond to region 1, subfield [3] to region 2, and subfield [4] to region 3 in Figure 2, respectively. Subfield [5] is added because of the obvious viscous effect in the boundary layers, although we were not able to visualize these layers with the smoke method used.

This is a general airflow pattern observed when the ventilation rate is low (approximately 5 to 10 air changes per hour). When the ventilation rate increases, the jet will penetrate further toward the opposite wall so that subfield [1] will expand and subfield [3] contract. For a given configuration and inside arrangement of a building, the whole flow field is dictated principally by the diffuser jet.

The above flow features, therefore, should be included in either a similitude model study or a numerical simulation of room air diffusion. In the similitude study, a scaling factor may be proposed individually for each subfield in which the flow is simpler to describe compared to the whole room, since complete similarity between a reduced-scale model and its prototype is difficult to maintain when both thermal buoyancy and internal obstructions are present in the building. The combination of all subfield models then produces a complete picture of the whole flow field. Such a subfield modeling method may result in a simpler mathematical description of ventilation flows, since some effects may be negligible in modeling each subfield.

Results of Reduced-Scale Physical Model Study

TABLE 2. Experimental Conditions[6]

Test #	T_w (°C)	T_i (°C)	U_i (m/s)	w_i (mm)	Q (m^3/s)	ΔT_a (°C)	Re	Ar ($\times 10^3$)
1	25	24.9	1.17	9.5	.011	0	1000	0
2	37	26.1	1.17	9.5	.011	7.6	1000	2.15
3	65	25.9	1.17	9.5	.011	9.8	1000	2.75
4	37	27.5	1.75	6.3	.011	5.7	1000	4.38
5	37	28.0	0.88	12.7	.011	4.5	1000	2.44
6	37	25.0	1.84	9.5	.018	3.4	1120	0.31
7	37	24.0	2.57	9.5	.025	3.1	1550	0.14

General Analysis of the Airflow Pattern

Seven tests were conducted in the 1/12th scale room (Table 2). The general airflow patterns for these tests were observed with the smoke wire method. They were characterized by a bent free air jet attached to the ceiling, a ceiling jet, and a large recirculating eddy (Figure 4). The air jet was bent due to the Coanda effect.

---

[6] All variables are defined in the list of symbols of this paper.

Figure 5a shows the measured mean velocity distribution for test 2. The decay of maximum jet velocity at measured sections (columns) downstream was clearly identified. The variation of locations at which the maximum velocity occurred indicated that the air jet was bent toward the ceiling due to the Coanda effect, traveled as a ceiling jet for some distance, and then separated from the ceiling. Meanwhile, the jet also expanded due to the entrainment of the ambient room air. The lowest velocity region was at the medium height level (y/H=0.41 to 0.66), which corresponded to the center of the large recirculating eddy. Air below the level of y/H=0.41 traveled in the opposite direction of the incoming air jet, forming a reverse flow. Velocities in this reverse flow are of the most concern because this region includes the occupied zone of typical rooms. It can also be seen that the velocity decreased as air traveled toward the diffuser side (from x/W=0.83 to x/W=0.06) in the reverse flow. This could be attributed to the retardation of the floor by viscous force and the further mixing with the internal heat load produced by heated water circulating through the pipes at the floor level.

Figure 5b shows the distribution of mean temperature. The low temperature region was around the diffuser due to the injection of cooler air, while the high temperature region was close to the floor due to the heat generated there. Temperature increased as the air traveled upstream in the reverse flow because of the heat transferred from the floor heat source.

It was intended to reproduce the general airflow pattern observed in the full scale rooms (Figure 3) in the reduced-scale building. However, to do this, very low diffuser air velocities needed to be maintained, and the room air velocities were even lower. The presently used smoke wire method was not applicable for flow visualization in such a slow ventilation flow, since the thermal buoyancy force exerted on the smoke due to the heat from the wire had a more important effect on the movement of the smoke compared to the room airflow pattern; thus, the smoke pattern could not represent the true flow pattern. In addition, the hot wire anemometer used was unable to sense such a low air velocity with enough certainty because of the effect of the natural convective heat transfer over the heated sensor probe. Therefore, the following discussion is limited to the flow patterns tested (Figure 4), which were characterized by higher than normal ventilation rates.

Effects of Thermal Buoyancy

Figure 6 shows the decay of maximum velocity in the jet for three water bath temperatures (T_w) while keeping the diffuser air velocity and opening width the same (tests 1, 2, and 3). When T_w increased and thereby the temperature difference between the room air and diffuser air (ΔT_a) increased, the maximum velocity (U_m) in the jet decayed faster and to a lower value.

A surprising phenomenon was that the maximum velocities in the jet measured in the section of x/W=0.06 were higher than the diffuser air velocity. Possibly this is because the section was within the initial region of the jet so that the horizontal velocity was equal to that at the diffuser outlet, while the ambient room air added a vertical velocity component to the jet, resulting in a higher total local maximum velocity in the jet. In other words, the air jet appeared to gain momentum for a short region upon entering the room from the room airflow

already established by the previous diffuser jet flow. Another explanation might be the Vena contract, which was approximately 25.4 mm into the room, and this is plausible since the diffuser had an abrupt geometry change at the outlet. The third possible explanation is that the hot wire anemometer has a temperature-compensation unit (a temperature sensitive resistor exposed to the flow) above and near the velocity sensor, and some interaction could occur between the thermal wake of the velocity sensor and the temperature-compensation resistor when there is a vertical velocity component, causing an artificially high reading.

Figure 6 also shows that increasing thermal buoyancy effect (i.e., the increases of ΔT_a) also increased the maximum velocity in the jet (U_m) at this section. All these made the jet flow in a ventilated room much more complicated than an isothermal free jet or wall jet in still ambient fluid. Further measurements are needed to investigate this phenomenon in detail.

The increased internal heat production decreased the average mean air velocity in the reverse flow region (Table 3). This seems to be contradictory to the results from the field measurement, where the thermal buoyancy due to internal heat sources appeared to increase the air velocities right above the sources. This is because the thermal buoyancy had a locally dominating effect in the low velocity region (region 2 in Figure 2) of the full-scale rooms, while in the reduced-scale model, the thermal buoyancy did not have a locally dominating effect but balanced part of the inertial effect so that a lower air velocity resulted in the reverse flow, compared to the isothermal flow case.

TABLE 3. Average Mean Velocity in the Reverse Flow for Different Thermal Buoyancy Effects*

x/W:	0.06	0.25	0.44	0.61	0.83	Average
ΔT_a=0°C	.14	.20	.27	.30	.24	.23
ΔT_a=7.6°C	.06	.14	.24	.28	.28	.20
ΔT_a=9.8°C	.07	.10	.21	.24	.24	.17

* Velocities are in m/s and are averages of data at y/H=0.03, 0.16 and 0.28

It was also observed with the smoke wire method that the attachment distance (L_a) increased and the separation distance (L_s) decreased due to the increased thermal buoyancy effect, when T_w increased (refer to Figure 4 for the definition of L_a and L_s).

Effect of diffuser opening width with constant ventilation rate

The effect of diffuser opening width was determined by varying the diffuser opening size while keeping the ventilation rate and water bath temperature constant (tests 2, 4, and 5). As shown in Figure 7, the thinner jet (i.e., smaller opening width) with higher diffuser air velocity decayed slower, resulting in a higher velocity at the section of x/W=0.833. This means that a thinner jet would penetrate further than a thicker jet in a ventilated room, even though the Reynolds number is the same.

The thinner jet also resulted in a higher average air velocity in the reverse flow (Table 4). This is in agreement with Ogilvie and Barber's (1989) result that floor airspeed increased with the jet momentum number (J), which is proportional to the product of ventilation rate and inlet air velocity ($J=QU_i/gV$).

It is often desirable to limit the airspeed in the occupied zone while achieving adequate air exchange and mixing. The above result suggests that the diffuser air velocity should only be maintained to a level that is just enough to ensure adequate air entrainment and keep the incoming air jet in the desired direction, since excessive diffuser air velocity will result in higher air velocity in the occupied zone (i.e., in the reverse flow).

TABLE 4. Average Mean Velocity in the Reverse Flow for Different Diffuser Opening Widths*

x/W:	0.06	0.25	0.44	0.61	0.83	Average
w=6.3 mm	.09	.14	.24	.25	.23	.19
w=9.5 mm	.06	.14	.24	.28	.28	.20
w=12.7 mm	.10	.16	.28	.26	.26	.22

* Velocities are in m/s and are averages of data at y/H=0.03, 0.16 and 0.28

In addition, the smoke pattern observed indicated that the thinner jet (i.e., less vertical thickness) had a smaller attachment distance. There were two reasons for this. First, the higher diffuser air velocity increased the pressure difference between the upper and lower edges of the jet, which caused the jet to bend toward the ceiling (i.e., the Coanda effect). Second, the higher diffuser air velocity caused the incoming air to be better mixed with the room air before it was exhausted, and as a result, the temperature difference between the inside and outside air was smaller (compare ΔT_a in Table 2 for tests 2, 4, and 5) so that there was less thermal buoyancy effect on the jet. The effect of varying diffuser opening width on the separation distance was not clearly shown by the smoke pattern. It would depend upon the relative magnitude of the inertial effect and thermal buoyancy effect. The inertial effect would increase the separation length while the thermal buoyancy effect would decrease it. Additionally, the viscous effect due to the presence of the ceiling would decrease the inertial effect.

Effect of Ventilation Rate

The effect of ventilation rate was evaluated by varying the ventilation rate while keeping the diffuser opening size and water bath temperature constant (tests 1, 6, and 7). As the ventilation rate increased, the Reynolds number, based on the diffuser opening width and diffuser air velocity, also increased. As a results, the air velocity in both the jet region and reverse flow region increased (Figure 8 and Table 5), as expected. However, the dimensionless velocity based on the diffuser air velocity (i.e., Average/U_i in table 4) decreased, which indicated that the dimensionless velocity also depended on the Reynolds number for the flow case studied. This is expected, because it is only for isothermal ventilation flows and where the diffuser Reynolds number is higher

than a threshold that the dimensionless velocity is independent of Reynolds number, as suggested by Pattie and Milne (1966), Timmons (1984), and others.

Additionally, flow visualization with the smoke wire method indicated that the attachment distance decreased with the increase of ventilation rate (essentially the diffuser air velocity), and the separation distance increased. This can be explained by the increased Coanda effect and increased inertial force relative to the thermal buoyancy force because of the increased diffuser air velocity.

TABLE 5. Average Mean Velocity in the Reverse Flow for Different Diffuser Air Velocities*

x/W:	0.06	0.25	0.44	0.61	0.83	Average	Average/U_t
Q=108.5 m^3/s	.06	.14	.24	.28	.28	.20	.172
Q=179 m^3/s	.11	.15	.24	.31	.27	.22	.119
Q=250 m^3/s	.11	.16	.28	.35	.32	.24	.093

* Velocities are in m/s

Summary and Conclusions

1. The velocity measurements and flow visualization in rooms with internal obstructions and heat sources suggested that the whole flow field may be divided into five types of subfields, and a subfield modeling method may be used for developing mathematical models of room air distribution in ventilated spaces.

2. Experiments in a reduced scale room were conducted for flow fields characterized by a turbulent horizontal jet directed along the ceiling and a large recirculating eddy. The following results were obtained:

(a) Increasing thermal buoyancy due to the floor heat source increased the decay rate of the maximum velocity in the diffuser air jet and decreased the average mean velocity in the reverse flow region, which included the occupied zone. It also increased the distance at which the jet attached to the ceiling and decreased the distance at which the jet separated from the ceiling.

(b) For the same ventilation rate, increasing the diffuser air velocity by reducing the diffuser opening size increased the air velocity in the reverse flow region, and the incoming air was better mixed with the room air before it was exhausted. Therefore, when it is desired to minimize airspeeds in the occupied zone, the diffuser air velocity should be kept just high enough to ensure adequate air mixing and to maintain the air jet traveling in the desired direction.

(c) Increasing ventilation rates by increasing the diffuser velocity, which means an increase in the diffuser Reynolds number, caused the air velocity in the occupied zone to increase. However, the ratio of the velocity in the occupied zone to the diffuser air velocity decreased. Therefore, air distribution in a ventilated building with internal heat production is

generally Reynolds number dependent, except for isothermal and highly turbulent flow.

LIST OF SYMBOLS

A= Area of the diffuser outlet (m^2)

Ar= Archimedes number defined as $\frac{\beta g w_1 \Delta T_a}{U_1^2}$

Ar_c= Corrected Archimedes number defined as $\frac{0.6A}{D}$ Ar

a= Constant in the velocity decay function of the air jet

b= Decay coefficient of the air jet

D= Characteristic dimension of a room, defined as $\frac{2WH}{W+H}$

g= Gravitational acceleration (m/s^2)

J= Jet momentum number defined as $\frac{QU_1}{gV}$

L_a= Attachment length of the air jet (Fig. 4), (m)

L_s= Separation length of the air jet (Fig. 4), (m)

Q= Ventilation rate (m^3/s)

q= Heat generated by from the floor (W/m^2)

R= Correlation coefficient

Re= Diffuser Reynolds number defined as $\frac{U_1 w_1}{\nu}$

SD= Standard deviation of velocities (m/s)

SDmax= Maximum standard deviation of velocities at measured points (m/s)

T_1 = Air temperature at the diffuser outlet (°C)

T_w= Water temperature in the water bath (°C)

U= Air velocity at the measured points (m/s)

U_1= Diffuser air velocity (m/s)

U_m= Maximum velocities in the jet at the measured sections (m/s)

Umax = Maximum of velocities at measured points (m/s)

Ur= Average velocity in the reverse flow region (m/s)

V= Room volume (m^3)

W= Width of the building (m)

w= Width of the inlet opening (m)

x= Horizontal coordinate (m)

y= Vertical coordinate (m)

ΔT= Temperature difference between room air and incoming air at the diffuser air for a measured point (°C)

ΔT_a= Average temperature difference between the room air and the incoming air at the diffuser

ΔTm= Maximum temperature difference between the room air and the incoming air at the diffuser (°C)

β= Thermal expansion coefficient (S/K)

ν= Kinematic viscosity (m^2/s)

Literature Cited

Anderson, R and Mehos, M. Evaluation of indoor air pollutant control techniques using scale experiments. ASHRAE IAQ 88, Atlanta, GA, 1988, pp. 193-208.

Baturin, V.V. Fundamentals of Industrial Ventilation. 3rd edition. Pergamon Press, Oxford, U.K, 1972.

Christianson, L.L. Building systems: Room Air and Air Contaminant Distribution. ASHRAE, Atlanta, GA, 1989.

Christianson, L.L., Riskowski, G.L., Zhang, J.S. and Koca, R. Predicting air velocity at the pig level. Proceedings of the International Livestock Environment Symposium, Toronto, 1988.

Furry, R.B. and Hazen, T.E. A constant temperature model of ventilation-dilution phenomenon. Transactions of the ASAE, 1967, 10(2):188-195.

Int-Hout, D. Physical modeling. In L.L. Christianson (Ed.), Building Systems: Room Air and Air Contaminant Distribution. ASHRAE, Atlanta, 1989.

Moog, W. Room flow tests in a reduced-scale. Trans. of ASHRAE, 1981, CH-81-17, No.4. 1162-1181.

Pattie, D.R. and Milne, W.R. Ventilation airflow patterns by use of models. Trans. of ASAE, 1966, 9(5):646-649.

Timmons, M.B. Internal air velocities as affected by the size and location of continuous diffuser slots. Trans. of ASAE, 1984a, 27(5):1514-1517.

Timmons, M.B. Use of physical models to predict the fluid motion in slot-ventilated livestock structures. Trans. of ASAE, 1984b, 27(2):502-507.

Yao, W.Z., Christianson, L.L. and Muehling, A.J. Air movement in neutral pressure swine buildings - similitude theory and test results. ASAE Paper 86-4532. Amer. Soc. Agr. Engr., St. Joseph, MI 49085-9659, 1986.

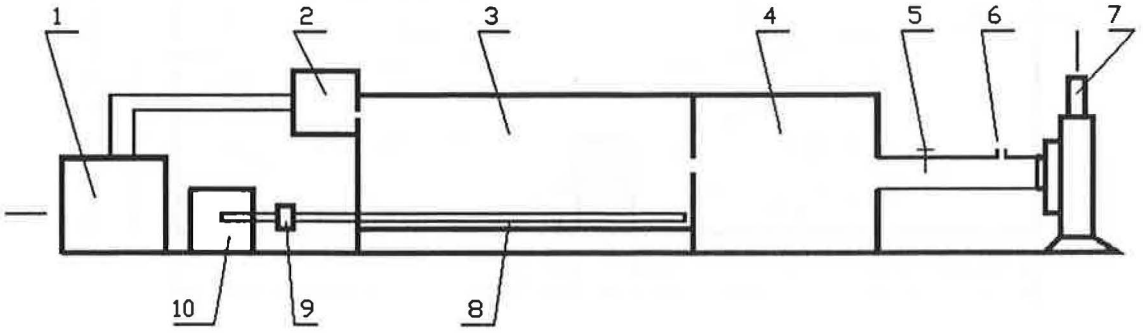

1 : Air conditioner 2 : Inlet duct 3 : 1/12th scale chamber 4 : Outlet plenum 5 : Valve
6 : Hole for measuring air flow rate 7 : Exhaust fan 8 : Water pipe 9 : Water pump
10: Constant temperature water bath

Fig. 1 Experimental set up for the 1/12th scale model building (chamber)

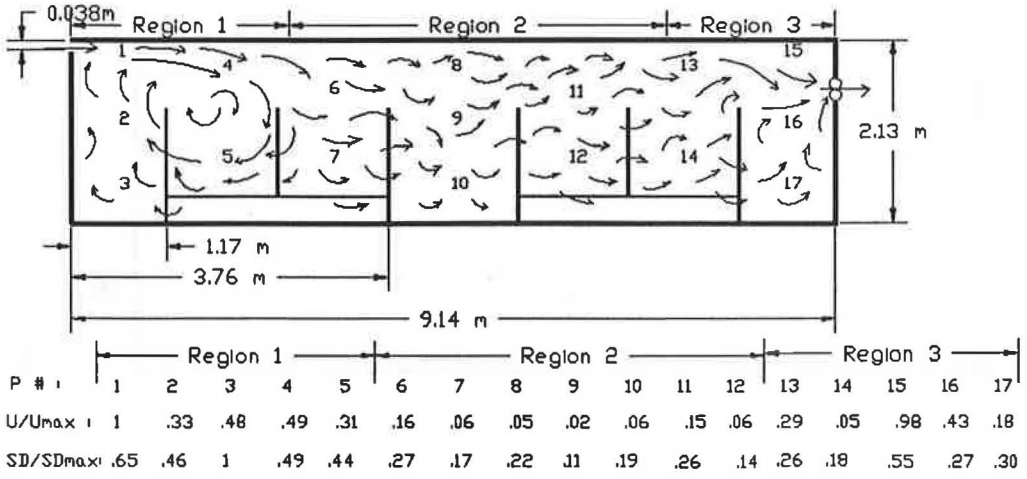

P # :	1	2	3	4	5	6	7	8	9	10	11	12	13	14	15	16	17
U/Umax :	1	.33	.48	.49	.31	.16	.06	.05	.02	.06	.15	.06	.29	.05	.98	.43	.18
SD/SDmax:	.65	.46	1	.49	.44	.27	.17	.22	.11	.19	.26	.14	.26	.18	.55	.27	.30

Fig. 2 Air distribution observed in a swine nursery room. Umax = 2.01 m/s, SDmax = 1.41 m/s. The internal obstructions are 1.4m height pens with about 70% slot openings on them.

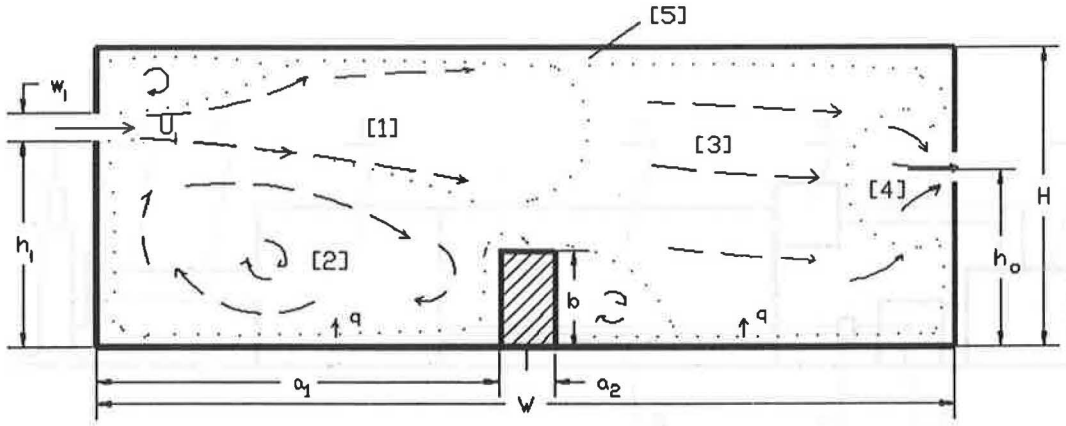

Fig. 3 General air flow pattern in a slot ventilated building with an obstruction.

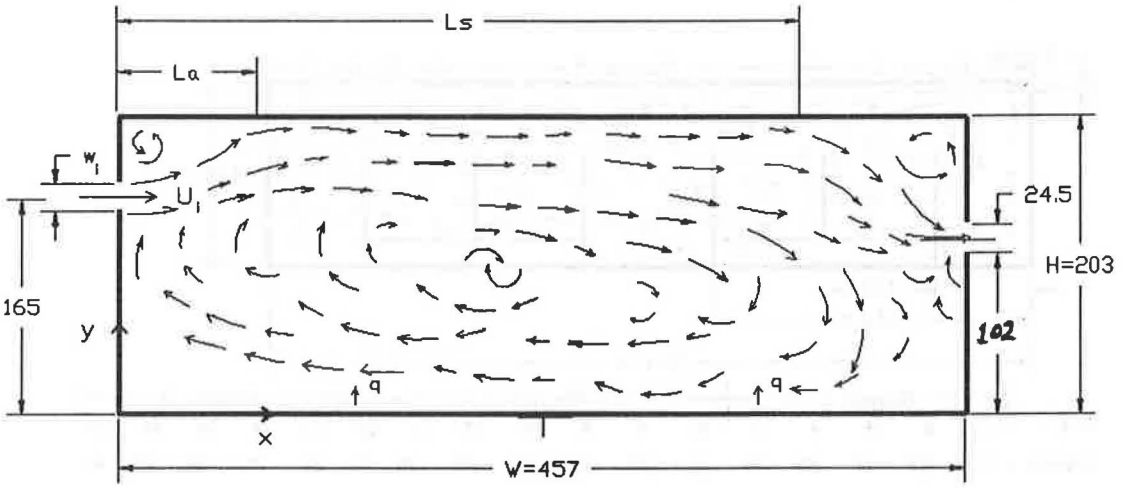

Fig. 4 Flow pattern studied in the 1/12th scale model building. All dimensions are in mm.

y/H	Column 1	Column 2	Column 3	Column 4	Column 5
1.00					
0.97	0.14	0.28	0.21	0.13	0.06
0.91	0.17	0.54**	0.51**	0.38	0.22
0.84	0.33	0.42	0.41	0.39**	0.35**
0.78 →	1.22**	0.21	0.33	0.33	0.31
0.72	0.11	0.09	0.22	0.28	0.29
0.66	0.00*	0.06*	0.16	0.21	0.25
0.59	0.03	0.10	0.14	0.19	0.21 →
0.53	0.08	0.10	0.11*	0.17	0.18
0.41	0.09	0.12	0.15	0.14*	0.14*
0.28	0.07	0.18	0.19	0.21	0.16
0.16	0.05	0.18	0.24	0.26	0.25
0.03	0.03	0.01	0.21	0.25	0.32
0	0.06	0.25	0.44	0.61	0.83 1
			x/W		

** : Maximum in the column * : Minimum in the column

Fig. 5a Velocity distribution (U/U_1) for test 2.
U_1=1.17 m/s, w_1=9.5 mm, ΔT_a=7.6 °C

y/H	Column 1	Column 2	Column 3	Column 4	Column 5
1.00					
0.97	0.39	0.44	0.51	0.56	0.51
0.91	0.37	0.37*	0.47	0.52	0.47*
0.84	0.32	0.38	0.45*	0.51*	0.51
0.78 →	0.21*	0.49	0.50	0.56	0.55
0.72	0.28	0.56	0.61	0.60	0.57
0.66	0.49	0.67	0.68	0.68	0.61
0.59	0.60	0.76	0.73	0.70	0.64 →
0.53	0.68	0.82	0.79	0.73	0.67
0.41	0.80	0.84	0.81	0.75	0.70
0.28	0.88	0.82	0.80	0.74	0.71**
0.16	0.89	0.88	0.79	0.76**	0.69
0.03	0.90**	1.00**	0.82**	0.73	0.67
0	0.06	0.25	0.44	0.61	0.83 1
			x/W		

** : Maximum in the column * : Minimum in the column

Fig. 5b Temperature distribution ($\Delta T/\Delta T_m$) for test 2.
U_1=1.17 m/s, w_1=9.5 mm, ΔT_a=7.6 °C, ΔT_m=12.0°C

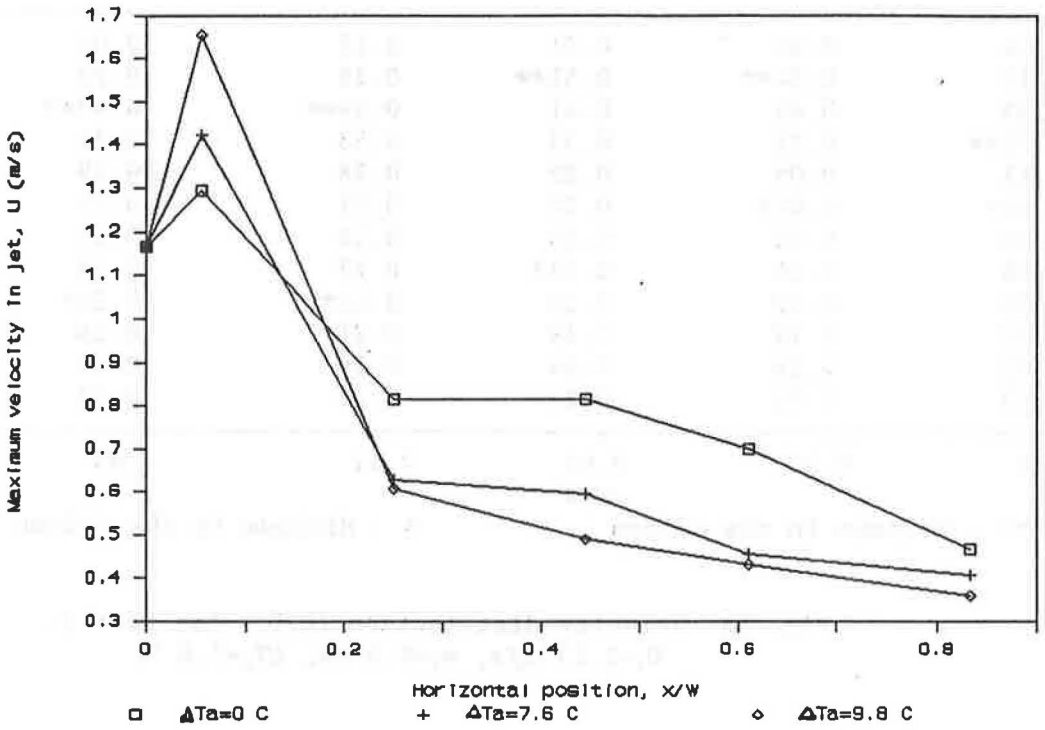

Fig. 6 Effect of thermal buoyancy on jet decay

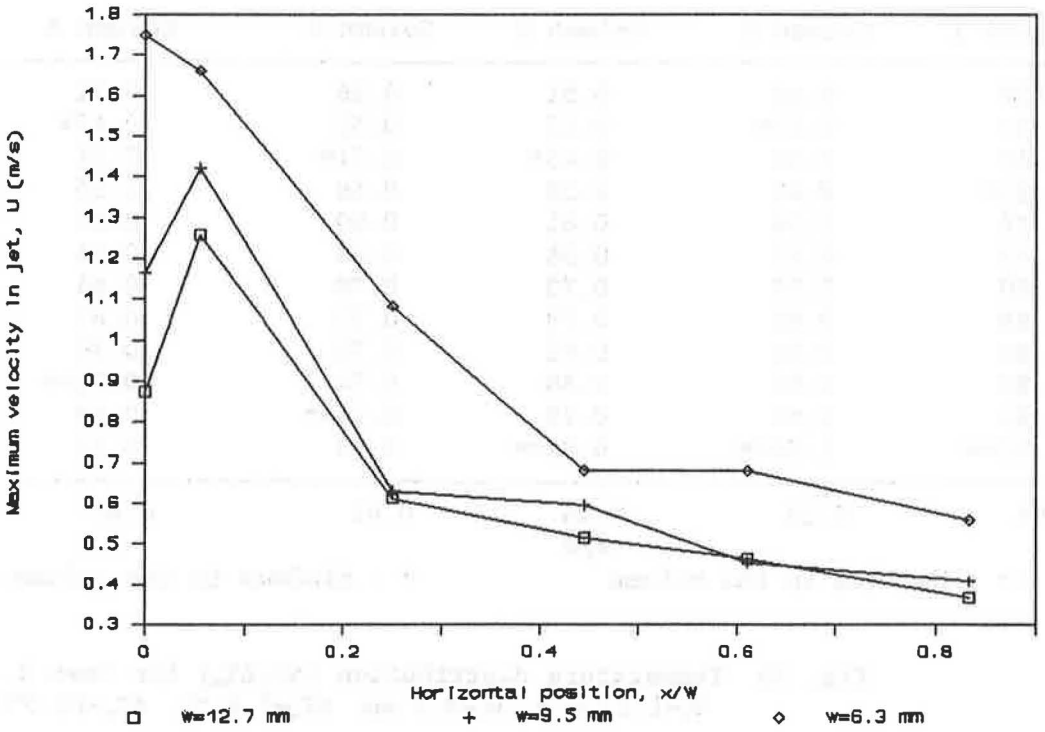

Fig. 7 Effect of inlet opening width on jet decay

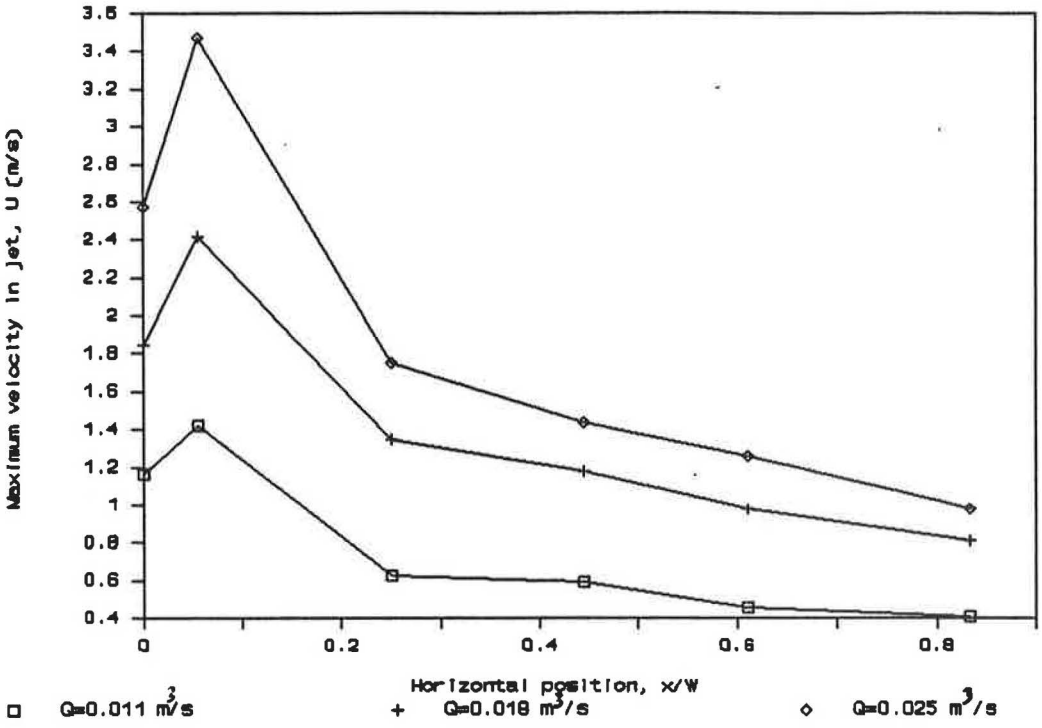

Fig. 8 Effect of ventilation rate on jet decay